Inorganica Chimica Acta, 36 (1979) 89–96

Equilibrium and Structural Studies of Nickel(II) Complexes of 1,4,8,11-Tetra-azacyclotetradecane and 1,4,8,11-Tetramethyl-1,4,8,11-Tetra-azacyclotetradecane in Co-ordinating Solvents and Nitromethane Solution: Isolation of some *Bis*-(Solvento)-Adducts of 1,4,8,11-Tetra-azacyclotetradecanickel(II) Perchlorate

NORMAN HERRON and PETER MOORE*

Department of Chemistry and Molecular Sciences, University of Warwick, Coventry CV4 7AL, U.K.

Received January 20, 1979

*Two isomers (*trans-*I and* trans-*III) of the diamagnetic, square-planar complexes* $[Ni(L_b)](ClO_4)_2$ *(L_b = 1,4,8,11-tetramethyl-1,4,8,11-tetra-azacyclotetradecane), and a single isomer (*trans-*III) of* $[Ni(L_a)](ClO_4)_2$ *(L_a = 1,4,8,11-tetra-azacyclotetradecane) have been investigated in co-ordinating solvents (H_2O, DMF, DMSO, MeCN) and in non-co-ordinating nitromethane. In aqueous solution, equilibrium constants (K) and related thermodynamic parameters (ΔH°, ΔS°) associated with diamagnetic ⇄ paramagnetic solvation equilibria ($[Ni(L)]^{2+} + nH_2O$ ⇄ $[Ni(L)(OH_2)_n]^{2+}$) have been determined from visible spectra and magnetic susceptibility measurements; at 298 K, K = 0.25, 1.05 and 1.14, $-\Delta H^\circ$/kJ mol^{-1} = 24 ± 2, 11 ± 2 and 44 ± 2, ΔS°/JK^{-1} mol^{-1} = −94 ± 10, −39 ± 10 and −143 ± 10 for complexes of* trans-*III-*L_a *(n = 2),* trans-*I-*L_b *(n = 1) and* trans-*III-*L_b *(n = 2) respectively. The structurally related* trans-*III-*$[Ni(L)]^{2+}$ *ions (L = L_a and L_b) form octahedral bis-solvento-adducts, whereas the* trans-*I-*$[Ni(L_b)]^{2+}$ *ion is sterically constrained such that it forms a five co-ordinate paramagnetic mono-(solvento)-adduct only. Spectrophotometric pH-titration of the aqua-complexes was undertaken, and their* pK_a*'s determined. Unstable solid* bis-*(solvento)-adducts of* $[Ni(L_a)](ClO_4)_2$ *with DMF, DMSO and MeCN have been isolated and characterized by a diffuse reflectance spectroscopy. The solid complexes with DMSO and MeCN were also examined by differential scanning calorimetry which confirms that MeCN is co-ordinated more strongly than DMSO, in agreement with the visible spectra of the solids. The rod-like MeCN molecule is also found to be a better ligand for* trans-*I-*$[Ni(L_b)]^{2+}$ *ion, solution visible and* ^1H *n.m.r. spectra showing complete formation of the* mono-*(acetonitrile) adduct, but only partial formation of* mono-*(solvento)-adducts in DMSO, DMF and* H_2O*. Low temperature* ^1H *n.m.r. studies of the paramagnetic, five-co-ordinate* trans-*I-*$[Ni(L_b)Cl]^+$ *ion indicates that it is trigonal bipyramidal (tbp) in nitromethane solution, but a distinction between square-pyramidal and tbp geometries is not possible from* ^1H *n.m.r. studies of the corresponding* $[Ni(L_b)(OH_2)]^{2+}$ *ion in aqueous solution.* ^{13}C *n.m.r. spectra of the three square planar diamagnetic* $[Ni(L)](ClO_4)_2$ *complexes (L = L_a or L_b) were also obtained in nitromethane solution.*

Introduction

Complexes of nickel(II) with the macrocycles L_a and L_b have been known for several years, yet no detailed comparisons of the properties of these closely related species have been reported. The complex $[Ni(L_b)](ClO_4)_2$ may exist as one of two, non-

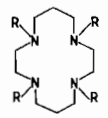

L_a: R=H
L_b: R=Me

interconvertible, square-planar isomers *trans*-I and *trans*-III [1] with tertiary-amine donor configurations (R,S,R,S) and (R,S,S,R) respectively [2, 3] (Fig. 1). The *trans*-I isomer readily forms five-co-ordinate

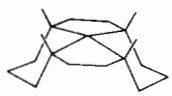

trans-I (R,S,R,S)

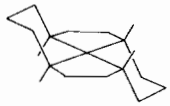

trans-III (R,S,S,R)

Fig. 1. Two isomers of $[Ni(L_b)](ClO_4)_2$.

*Author to whom correspondence should be addressed.

adducts with donor solvents or unidentate anions [3]. The exact structure of these species has been the subject of some debate, crystallographic evidence suggesting a square-pyramidal geometry [4, 5], whilst ^{13}C n.m.r. evidence for analogous zinc(II) complexes indicates fluxional, trigonal-bipyramidal species in solutions [5]. The *trans*-III isomer frequently ligates on axis to produce an octahedral complex, although five-co-ordinate species are also known with strong ligands such as the $[CN]^-$ ion [2]. The acetonitrile solvent exchange rates for solvates of both isomers of $[Ni(L_b)](ClO_4)_2$ have been measured [6] and the results interpreted in terms of very different exchange mechanisms. The *trans*-I isomer exchanges by an associative mechanism which is consistent with a trigonal bipyramidal ground state, whereas the *trans*-III isomer displays normal dissociative kinetics as expected for an octahedral complex. Clearly the conformation of the macrocycle in these two isomers markedly affects their overall properties, and so we have undertaken a comparison of other physical and chemical properties of the complexes which would be predicted to obviate the modifying effects of macrocycle conformation.

As a control and extension to this comparison, the parent complex $[Ni(L_a)](ClO_4)_2$ has been investigated. This complex adopts a *trans*-III (*R, S, S, R*)-type square-planar geometry [7] (Fig. 1), and axially ligates with halide ions to give octahedral species. Until recently it was thought that these octahedral species, and the square-planar complex itself, dissolved in water (and all other donor solvents) to give a solution containing purely diamagnetic square-planar unsolvated species. However, it has since been shown that such solutions contain a small percentage of a paramagnetic octahedral diaquo complex [8] in equilibrium with the square-planar species. The complex $[Ni(L_a)](ClO_4)_2$ differs from the equivalent L_b complex in that with L_a inversion of the unmethylated co-ordinated amine donors, and hence interconversion of isomers *trans*-I and *trans*-III, is permissible.

A comparison of the three nickel(II) complexes, two with L_b (*trans*-I and *trans*-III) and one with L_a (*trans*-III), therefore not only allows an estimation of the effects of macrocycle conformation, but also that of tertiary *versus* secondary amine donors on the properties of a closely related series of nickel(II) complexes. This work forms part of our investigation into the co-ordination properties of simple macrocyclic ligands [9, 10].

Experimental

The two isomers of $[Ni(L_b)](ClO_4)_2$, *trans*-I and *trans*-III, were prepared following published procedures [2, 3], as was the complex $[Ni(L_a)](ClO_4)_2$ [11]. All three complexes were recrystallized and dried *in vacuo* over P_2O_5. Purity was checked by nickel elemental analysis: $[Ni(L_b)](ClO_4)_2$, calculated: 11.42%. Found: *trans*-I, 11.43%; *trans*-III, 11.20%: $[Ni(L_a)](ClO_4)_2$. Calculated: 12.88%. Found: 12.86%. *Bis*-(solvento)-complexes of $[Ni(L_a)](ClO_4)_2$ may be obtained by preparing hot saturated solutions in solvents such as acetonitrile, dimethyl sulphoxide (DMSO) and dimethylformamide (DMF). Well formed, crystalline solids precipitate from such solutions on cooling and may be filtered under dry nitrogen. All three compounds readily lose co-ordinated solvents when washed with most common solvents, reverting to the orange square-planar complex. Even in dry nujol, the most stable acetonitrile complex undergoes slow solvent loss. This instability of the solvento-adducts to both washing and pumping to remove excess solvent prevented the isolation of analytically pure complexes. Analyses of the complexes obtained are given in Table I.

Variable temperature 90 MHz ^1H and 22.628 MHz ^{13}C n.m.r. spectra were recorded with a Bruker WH90 F.T. spectrometer, the temperature being controlled by a standard Bruker temperature unit capable of holding selected temperatures to ±0.5 °C. Temperatures were accurately established using a calibrated Comark thermocouple. All chemical shifts are quoted in ppm on the δ scale referenced to an internal standard. ^1H n.m.r. samples for the paramagnetic susceptibility study by the Evans [12] method were of fixed ionic strength, as were solutions for the parallel visible spectroscopic studies; ionic strengths are quoted in text.

Infra-red spectra were recorded with a Perkin Elmer 457 spectrometer as nujol mulls with CsI

TABLE I. Elemental Analyses for *Bis*-(solvento-adducts of $[Ni(L_a)](ClO_4)_2$.

Complex	% Ni		% C		% N		% H	
	required	found	required	found	required	found	required	found
$[Ni(L_a)(CH_3CN)_2](ClO_4)_2$	10.88	10.57	31.1	30.3	15.6	15.0	5.56	5.62
$[Ni(L_a)(DMSO)_2](ClO_4)_2$	9.57	8.32	27.4	27.5	9.1	6.6	5.87	6.00
$[Ni(L_a)(DMF)_2](ClO_4)_2$	9.73	7.95	31.8	34.5	13.9	14.6	6.30	6.84

windows. Uv–visible spectra were recorded in solution with either a Cary 14 or Unicam SP800 spectrophotometer, and as powdered solids, using the diffuse reflectance technique with the SP890 attachment to the latter instrument. Variable temperature solution visible spectra were measured in the nitrogen flushed thermostatted compartment of the Cary 14 spectrometer, temperatures being established by immersion of an alcohol thermometer (±0.05 °C) into the sample solution. Differential scanning calorimetry was performed with a Du Pont 900 Differential Thermal Analyser with the sample enclosed in a nitrogen atmosphere. The pH of solutions during pK_a determinations were measured using a Radiometer PHM64 Research pH meter calibrated with standard buffer solutions pH 4.00, 7.00 and 9.00. pH's were adjusted with 1 mol dm^{-3} KOH. Metal analyses were performed with a Varian AA6 atomic absorption spectrometer.

Results and Discussion

All three complexes, two of $[Ni(L_b)](ClO_4)_2$ and one of $[Ni(L_a)](ClO_4)_2$ dissolve in water to give a mixture of diamagnetic square-planar and paramagnetic solvated species. Visible spectra of the L_b complexes clearly show absorption bands associated with the paramagnetic species, but with L_a such bands are only directly observed for saturated solutions in long path length (4 cm) cells. The spectra are listed in Table II and from the extinction coefficients it can be seen that the *trans*-I isomer (Fig. 2) of the complex formed by L_b gives a five-co-ordinate *mono*-(solvento)-adduct, whereas both of the *trans*-III isomers (Fig. 1) of L_a and L_b form octahedral *bis*-solvento adducts. Variable temperature spectra, such as that shown in Fig. 2, for all three complexes in water confirm the presence of a diamagnetic $\rightleftarrows$ paramagnetic equilibrium, with higher temperatures favouring the diamagnetic state in all three cases. Addition of the inert electrolyte $NaClO_4$ has the same

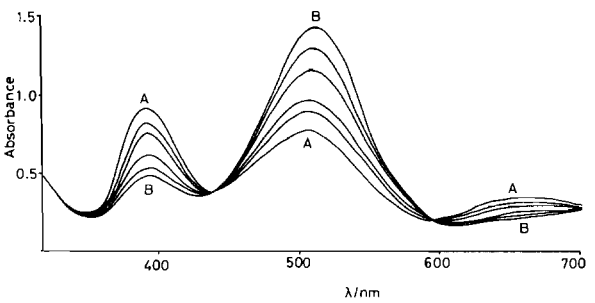

Fig. 2. Variable temperature visible spectra of 1.12×10^{-2} mol dm^{-3} *trans*-I $[Ni(L_b)](ClO_4)_2$ in H_2O. Temperatures are 279.7, 287.8, 296.7, 314.4, 322.5, 332.2 K in going from A to B.

effect as increasing temperature (ions of the $NaClO_4$ are thought to compete for the water molecules co-ordinated to the nickel(II) ion [13]) and limiting spectra of the pure square-planar species may be recorded in concentrated $NaClO_4$ solutions. Molar extinction coefficients of the pure diamagnetic species are then obtained as L_b; *trans*-I $\epsilon_{510} = 143$, *trans*-III $\epsilon_{494} = 73$ dm^3 mol^{-1} cm^{-1} and L_a: $\epsilon_{448} = 68$ dm^3 mol^{-1} cm^{-1}.

Using these values of ϵ for the square-planar complexes, the percentages of diamagnetic and paramagnetic solvated species may be determined in variable temperature visible spectra. In this way, equilibrium constants (K at I = 0.2 mol dm^{-3} $[Na(ClO_4)]$) for equilibria (1) may be established, and the temperature variations of ln K are plotted in Fig. 3. As an additional check on these values, estimates

$$[Ni(L)](ClO_4)_2 + nH_2O \overset{K}{\rightleftharpoons} [Ni(L)(OH)_2)_n](ClO_4)_2 \quad (1)$$

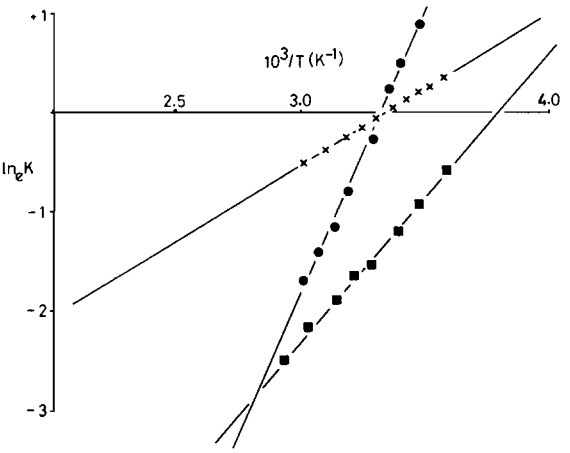

Fig. 3. Plot of ln K *vs.* 1/T for *trans*-I L_b (X); *trans*-III L_a (■); *trans*-III L_b (●) complexes of nickel(II), from visible spectral data.

of K were also obtained from ^1H n.m.r. susceptibility studies at the same ionic strength following the method of Evans [12]. Assuming a magnetic moment of 3.3 Bohr magnetons for the paramagnetic solvento complexes of L_b [2, 3] and 3.1 Bohr magnetons for the complex of L_a [14], then the measured magnetic moment gives directly the percentage of the paramagnetic species present. Variable temperature studies, therefore, allow an equivalent (yet complementary) set of equilibrium data to be obtained. Values of K, ΔH° and ΔS° for the equilibria derived from all sources are listed in Table III, and good agreement between the two methods is observed.

The normalised values of $-\Delta H^\circ$ in Table III (which refer to ligation by a single solvent molecule) are seen to be larger for the *trans*-III isomer of L_b

TABLE II. Visible Spectral Data for the Complexes in Aqueous Solution at 298 K.

Complex	Isomer	λ_{max}/nm (ϵ/dm^3 mol^{-1} cm^{-1})
$[Ni(L_a)](ClO_4)_2$	*trans*-III	650(<1), 448(59), 330(<1)
$[Ni(L_b)](ClO_4)_2$	*trans*-I	654(32), 510(70), 391(112)
$[Ni(L_b)](ClO_4)_2$	*trans*-III	494(27), 367(10)

than for the *trans*-III and *trans*-I complexes of L_a and L_b respectively. Previous workers [8] have pointed out that enthalpic trends such as those observed here may be ascribed to the changes in the ionic radius of the nickel(II) ion in going from low- to high-spin states. Such a conversion is associated with an increase of the optimum Ni-N bond length (1.91 → 2.07 Å) [15] and this change is most readily accommodated by *trans*-I complex, such as that of L_b, where the nickel(II) ion is not constrained in the plane of the four amine donors (Figure 1). Complexes with the *trans*-III geometry, on the other hand, must have the nickel(II) ion in the macrocyclic ligand plane (Fig. 1) and so rearrangement of the Ni–N bonds is opposed by the cyclic nature of the ligands. The L_b ring would be expected to oppose this change more strongly than L_a since rearrangement of the amine donors of L_b necessitates additional movement of methyl groups which are absent in L_a. This extra motion required in the case of both L_b complexes will, therefore, tend to increase the enthalpic barrier to the low- to high-spin conversion relative to the complex with L_a. If it is assumed that both macrocycles favour the smaller, low-spin nickel(II) ion, then the above observations explain the observed enthalpic trend. The entropies of reaction are all negative as expected for adduct formation. The entropy trend may be interpreted as reflecting the steric repulsions between the alkyl portions of the macrocycle and the co-ordinated water molecule(s) [8]. The *trans*-I complex of L_b has one very open face (Figure 1) (although surrounded by the four methyl groups) which quite readily accepts a water molecule. The *trans*-III isomers of L_a and L_b, however, have both faces partially blocked by the alkyl backbone of the six-membered chelate rings (Figure 1). In addition, the methyl groups of L_b increase this steric crowding still further, such that the complex of L_b has the greatest steric repulsion and therefore the most negative value of $\Delta S°$.

As a further exploration of the effects of macrocyclic ligands upon the properties of complexes, the pK_a of the co-ordinated water molecules in the aquo complexes discussed above were estimated by spectrophotometric pH titration. Such a titration is illustrated in Fig. 4 for *trans*-I-$[Ni(L_b)(OH_2)]^{2+}$ ion,

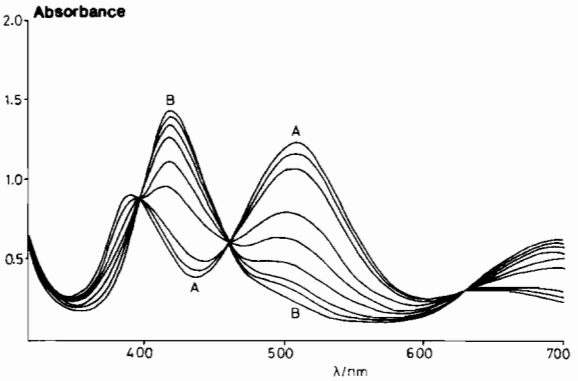

Fig. 4. Spectrophotometric pH titration of 1.12×10^{-2} mol dm^{-3} *trans*-I $[Ni(L_b)](ClO_4)_2$ in H_2O. (I = 1.04 mol dm^{-3}, T = 298 K). pH 6.43, 9.47, 10.02, 10.84, 11.22, 11.52, 11.72, 11.94, 12.96 in going from A to B.

and all three complexes gave good isosbestic points indicating the titrations are simple one step processes. The salient data from the titrations are listed in Table IV. The bright green product of the reaction of the *trans*-III complex of L_b has a spectrum which clearly suggests that it is a five co-ordinate mono-hydroxy

TABLE III. Thermodynamic Data at 298 K (I = 0.2 mol dm^{-3} [$NaClO_4$]) for the Diamagnetic to Paramagnetic Conversion of Nickel(II) Complexes of L_a and L_b in Aqueous Solution.

Macrocycle	Isomer	Method used	K	$-\Delta H°$/kJ mol^{-1}	$+\Delta S°$/JK^{-1} mol^{-1}	Normalised Values[b]	
						$-\Delta H°$/kJ mol^{-1}	$+\Delta S°$/JK^{-1} mol^{-1}
L_b	*trans*-I	Visible spectra	1.05	12.2 ± 1.6	−41 ± 9	12.2	−41
L_b	*trans*-I	Evans susceptibility	0.99	10.7 ± 2.0	−36 ± 10	10.7	−36
L_b	*trans*-III	Visible spectra	1.14	43.8 ± 1.6	−146 ± 10	21.9	−73
L_b	*trans*-III	Evans susceptibilty	2.90	44.4 ± 2.0	−140 ± 10	22.2	−70
L_a	*trans*-III	Visible spectra	0.25	24.0 ± 1.5	−91 ± 8	12.0	−45
L_a[a]	*trans*-III	Visible spectra	0.43	22.7 ± 1.7	−84 ± 8	11.3	−42
L_a	*trans*-III	Evans susceptibility	0.16	24.1 ± 1.8	−96 ± 10	12.0	−48

[a]From reference 8, I = 0.1 mol dm^{-3}. [b]These values refer to ligation by a single solvent molecule.

TABLE IV. Data from the Spectrophotometric pH Titration (with KOH) of the Nickel(II) Complexes of L_a and L_b in Aqueous Solution (298 K, I = 1.0 mol dm^{-3} [KNO_3]).

Macrocycle	Isomer[a]	Isosbestic Points, λ/nm	Final Product of Titration λ/nm (ϵ/dm^3 mol^{-1} cm^{-1})	pK[b]
L_b	*trans*-I (n = 1)	397, 461, 630	419(127), ~700(57)	10.82 ± 0.17
L_b	*trans*-III (n = 2)	452, 551	398(132), 643(61)	11.94 ± 0.07
L_a	*trans*-III (n = 2)	383, 512	350(18), 532(13)	13.67 ± 0.15

[a]See Figure 1. [b]Overall pK for the reactions: $[Ni(L)(OH_2)_n]^{2+} \overset{K}{\rightleftharpoons} [Ni(L)(OH)_n]^{(2-n)+}$.

species (*i.e.* deprotonation of one co-ordinated water molecule causes immediate loss of the second water molecule).

The ability of the *trans*-III complex of L_b to co-ordinate a single ligand to become five co-ordinate has been noted previously with Cl^- [16] and CN^- [2] ions, but in both cases addition of excess ligand produces normal octahedral species (addition of CN^- ion leads to decomposition). With hydroxide ion, however, the five co-ordinate complex appears stable in the presence of excess base. An explanation of this behaviour is tentative, but it would seem reasonable that co-ordination of one strong ligand to the nickel ion may well displace it from the plane of the four amine donors since the $[OH]^-$ ion may be restricted from approaching in a normal octahedral mode by the alkyl backbone and methyl groups of the macrocycle. Thereafter, co-ordination of a second ligand in a *trans*-position to the first will be sterically impossible, the site being blocked by the macrocycle itself.

The pK_a values of the three complexes (Table IV) lie in the order *trans*-I L_b < *trans*-III L_b < *trans*-III L_a, and it is significant that this is the same order as the in-plane ligand-field strengths (as reflected in the λ_{max} of the square-planar species; 510, 494, 448 nm respectively [17]). Such a correlation is reasonable since it has been found that for nickel(II) macrocycle complexes the larger is the in-plane ligand-field strength of the macrocycle, the weaker is the axial field strength [17, 18]. Thus the complex with the most strongly co-ordinated macrocycle, L_a would be predicted to have the most weakly co-ordinated water molecules. This then implies less weakening of the O–H bonds of the co-ordinated water with a consequently higher pK_a as observed.

One previously unreported property of the complex $[Ni(L_a)](ClO_4)_2$, noted during this work, is its ability to axially solvate to produce *bis*-(solvento)-adducts with donor solvents MeCN, DMSO and DMF. The compounds may be isolated as solids (green, mauve and grey crystals respectively) and it appears that the axial solvation of the square-planar cation can only occur effectively when such an interaction is stabilised by crystal forces (solutions of the cation in the appropriate solvents remain orange although some solvation occurs since ϵ_{max} of the square-planar band is reduced in the order DMSO < DMF < MeCN, *i.e.* MeCN co-ordinates most strongly). All three adducts are unstable with respect to solvent loss (see experimental) and must be stored sealed under dry nitrogen or in an atmosphere of the appropriate solvent. Diffuse reflectance spectra of fresh samples of each complex are listed in Table V and show three bands (the longest wavelength band being due to one component of the tetragonally split lowest energy band, $^3T_{2g} \leftarrow {}^3A_{2g}$ [14, 19]) corresponding to a distorted *trans*-octahedral environment for the nickel-(II) ion.

The absorption maxima of these three solvent-compounds are seen to undergo bathochromic shift in changing from the weakest donor to the strongest; λ_{max} DMSO > DMF > MeCN. This series is the reverse of that expected based purely on donor strength [20] and it is significant that adducts with water and pyridine are not isolable, despite their comparable donor strengths. The acetonitrile and DMSO complexes were subjected to differential scanning calorimetry which confirm that both adducts are *bis*-(solvento)-species and that the acetonitrile is more firmly bound than the DMSO. The acetonitrile adduct displays a single endotherm at 82 ± 1 °C, a sample weight loss corresponding to the removal of exactly two equivalents of acetonitrile and a desolvation energy corresponding to 45 ± 5 kJ per mole of solvent. The DMSO adduct showed similar behaviour with an endotherm at 135 ± 2 °C with a desolvation energy corresponding to 10 ± 5 kJ per mole of solvent. All the available data on the solvento adducts therefore suggest that the reversal of normal donor behaviour (*i.e.* the weakest donor molecule, MeCN, is most strongly bound) is a direct consequence of the steric limitations to complex formation imposed by the macrocycle. It is then less surprising that the least hindered, 'rod-lile' donor, MeCN, can most readily enter the co-ordination sphere of the nickel(II) ion.

All three nickel(II) complexes of L_a and L_b were also examined by n.m.r. spectroscopy. In dry nitromethane, they give ^{13}C n.m.r. spectra consistent with their proposed geometries (Table VI) and display no

TABLE V. Diffuse Reflectance Spectra of the *Bis*-(solvento-adducts of $[Ni(L_a)](ClO_4)_2$.

Solvent	$^3T_{2g} \leftarrow {}^3A_{2g}$/nm	$^3T_{1g}(F) \leftarrow {}^3A_{2g}$/nm	$^3T_{1g}(P) \leftarrow {}^3A_{2g}$/nm
CH_3CN	620 ± 10	472 ± 2	322 ± 2
DMSO	650 ± 5	520 ± 2	343 ± 2
DMF	630 ± 10	500 ± 5	335 ± 2

TABLE VI. ^{13}C N.m.r. Chemical Shifts for Complexes of Nickel(II) with L_a and L_b in $[^2H]_3$-nitromethane (shifts relative to internal dioxan, $\delta \simeq 67.3$ ppm).

Macrocycle	Isomer	Temperature/K	Shift δ/ppm
L_b	*trans*-I	303 → 233	56.41, 53.61, 39.74, 20.54
L_b	*trans*-III	303	59.82, 58.26, 45.91, 22.12
L_a	*trans*-III	298 → 263	50.86, 49.01, 26.66

dynamic behaviour on cooling below room temperature. (The *trans*-III complex of L_b is too insoluble to make low temperature accumulations worthwhile). One question, unanswered by any of the preceding data, is whether the five co-ordinate complex ions of the type *trans*-I $[Ni(L_b)X]^{n+}$ (n = 1 or 2) exist in solution as a square-pyramid or a trigonal-bipyramid. Both geometries have precedent for such complexes [5], but direct n.m.r. evidence for macrocycle folding to a trigonal-bipyramid is, in this case, intrinsically difficult to obtain because of the paramagnetism of the five co-ordinate species. However, a variable temperature paramagnetic ^1H n.m.r. study of the complex $[Ni(L_b)Cl]ClO_4$ in dry nitromethane is illustrated in Fig. 5. At high temperatures (340–370

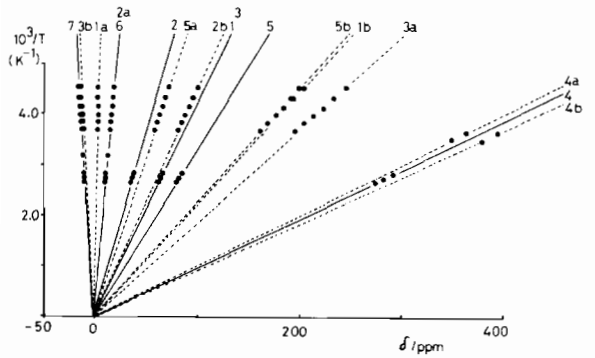

Fig. 5. Temperature dependence of the paramagnetic ^1H shifts of *trans*-I $[Ni(L_b)Cl]ClO_4$ in nitromethane (shifts referenced to internal TMS; for assignments see Fig. 6).

K) there are seven contact-shifted resonances present as expected for a square-pyramidal geometry (Fig. 6a). The relative integrals are 6:2:1 [Fig. 6a; resonances 1, (2–5) and (6–7) respectively] with one of the resonances appearing beneath the single N-Me resonance. The shifts of these high temperature

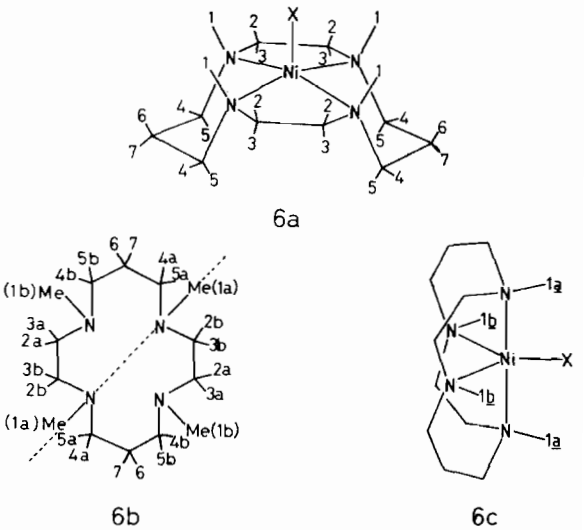

Fig. 6. Square pyramidal (6a) and trigonal bipyramidal (6c) geometries for $[Ni(L_b)X]^+$ ions. In 6c the macrocycle is folded about the dashed line shown in 6b.

resonances show an expected Curie-law temperature dependence as illustrated by the solid lines in Fig. 5, and upon cooling below 340 K five of the seven resonances (including the N-Me resonance) broaden and then split into two new resonances [labelled a and b in Figs. 5 and 6b], whose shifts then show a Curie-law temperature dependence down to the freezing point of the solvent (220 K). This is illustrated by the dashed lines in Fig. 5.

This complex behaviour is exactly equivalent to that observed in the ^{13}C n.m.r. spectra of other $[M(L_b)X]^+$ ions (*e.g.* M = Zn^{II}, Cd^{III}, Hg^{II}) [5, 6]. One interpretation [5] is that the macrocycle is folding about an axis through diagonally opposed N-atoms (dashed line in Fig. 6b) so as to produce a trigonal bipyramidal (tbp) complex (Fig. 6c). The

only alternative explanation, namely that the torsional motion of the backbone carbon frameworks is frozen out in a square-pyramidal complex (6a) can be dismissed since one would expect to see such behaviour in the low temperature ^{13}C n.m.r. spectrum of the square-planar $[Ni(L_b)]^{2+}$ ion. Since there is no evidence for a dynamic process of this type for $[Ni(L_b)]^{2+}$, we believe that folding of the macrocycle to produce a tbp geometry at low temperatures is the more likely explanation, and the very large splittings observed for five of the resonances at low temperatures (Fig. 5) is also consistent with this view. The two resonances which do not split at low temperatures are readily assigned to the central methylene group of the six-membered chelate rings (Fig. 6b), and their relatively small contact shifts are consistent with this interpretation since they are furthest from the paramagnetic ion. The other assignments in Fig. 5 are only tentative, being based upon approximate metal-hydrogen distances in molecular models.

If the splittings of the five resonances shown in Fig. 5 did arise from a slowing of the dynamic conformational effects within the two five-membered chelate rings of a square-pyramidal complex, then this implies that the process is synchronous between the equivalent chelate rings so as to maintain a two-fold symmetry axis and to prevent splitting of the two resonances from the central methylene group of the six-membered chelate rings. This requirement is not fulfilled in any crystal structure of complexes of this type [4, 5] which show the two five-membered rings to be related by mirror symmetry which *would* be expected to cause splitting of these resonances. Further evidence in favour of the proposed tbp geometry comes from the previously reported [6] acetonitrile solvent exchange kinetics of *trans*-I-$[Ni(L_b)(MeCN)]^{2+}$ ion which show an associative mechanism. The transition-state for this process is most likely to be *cis*-octahedral which is more readily accommodated by a tbp rather than a square-pyramidal geometry. It would seem, therefore, that *trans*-I complexes of L_b with Ni^{II}, Zn^{II}, Cd^{II} and Hg^{II} are rapidly interconverting trigonal bipyramids in solution. The crystalline structures, however, are invariably square-pyramidal [4, 5].

^1H n.m.r. spectra of $[Ni(L_b)](ClO_4)_2$ in D_2O/HOD also show seven contact-shifted ligand resonances between 270 and 370 K, the least broadened resonance (upfield of DSS) showing a small splitting (approximately a doublet, J *ca.* 19 Hz at 298 K) due to coupling with the non-equivalent hydrogen atom attached to the same central methylene carbon atom of the six-membered chelate ring (6 and 7, Fig. 6a), and with longer range couplings to the neighbouring hydrogen atoms (4 and 5) unresolved. The seven resonances broaden on cooling but do not split in the temperature range investigated, and the shifts do not follow a Curie-law temperature dependence because of the rapid equilibrium between four-co-ordinate diamagnetic and five-co-ordinate paramagnetic species discussed previously (Table III). The temperature dependence of the chemical shifts is illustrated in Fig. 7, and by using the previously determined equilibrium constants to determine the concentration of paramagnetic species present (and hence to calculate its shift since the observed shift is a weighted average of those for the diamagnetic and paramagnetic species, the water exchange being very rapid), the Curie-law dependence of the calculated shift for the paramagnetic species is restored as shown in Fig. 7. Since the weighted average shifts are necessarily less than those observed for the entirely paramagnetic chloro-complex, and because the lowest temperature attainable in D_2O is

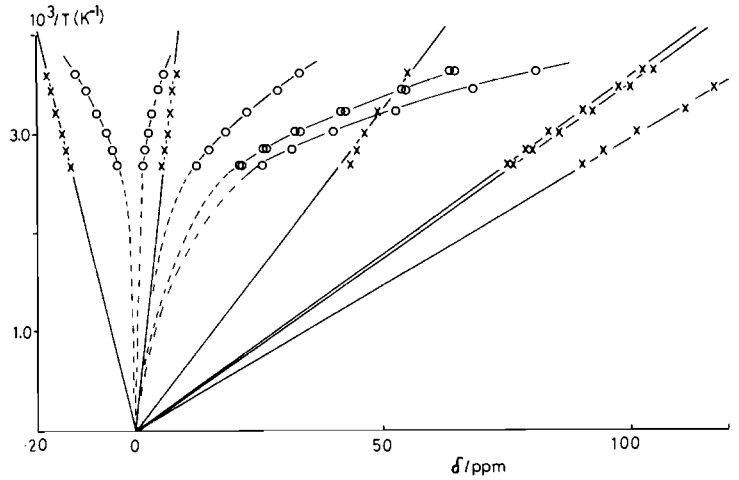

Fig. 7. Temperature dependence of six of the seven (see Fig. 6a) paramagnetic ^1H shifts of *trans*-I-$[Ni(L_b)(OH_2)](ClO_4)_2$ in H_2O (shifts referenced to DSS) (O = observed shift, X = shift corrected for equilibrium K). The seventh resonance has been omitted for clarity and has δ = 75 ppm at 370 K.

higher than that achieved with the chloro-complex in CD_3NO_2, it proved impossible to cause the seven ligand resonances of the aquo-complex to broaden and split as observed for the chloro-complex. A distinction between trigonal-bipyramidal and square-pyramidal geometries is, therefore, more difficult to establish in this case. However, there seems no reason to suggest why the chloro- and aquo-complexes might have different geometries and a tbp structure is favoured for both.

Conclusions

The data discussed here illustrates how simple conformational and substitutional effects within a macrocycle may modify the overall behaviour of the resultant complex with a metal ion. Steric and electronic effects such as those described in this work bear a similarity to the biochemical modification of metal ion properties in enzyme and metalloprotein chemistry and in this sense the macrocycles discussed above provide simple models for these complex biomolecules. In addition, the observed, systematic modification of the properties of macrocycle complexes is relevant to our research into the sequestring capabilities of macrocyclic ligands for the toxic heavy metal ions, Cd(II), Hg(II) and Pb(II). In this latter regard, the work of this paper has been extended to the exploration of complexes of L_a and L_b with such metal ions, and this work is in the process of publication.

Acknowledgments

We thank the M.R.C. and S.R.C. for support (to P.M.) and the S.R.C. for a studentship (to N.H.). We are also grateful to Courtaulds Ltd. (Coventry) for assistance with the differential scanning calorimetry experiments.

References

1 The nomenclature used here was first introduced by B. Bosnich, C. K. Poon and M. L. Tobe, *Inorg. Chem., 4,* 1106 (1965).
2 F. Wagner and E. K. Barefield, *Inorg. Chem., 15,* 408 (1976).
3 E. K. Barefield and F. Wagner, *Inorg. Chem., 12,* 2435 (1973).
4 M. J. d'Aniello Jr., M. T. Morella, F. Wagner, E. K. Barefield and I. C. Paul, *J. Am. Chem. Soc., 97,* 192 (1975).
5 N. W. Alcock, N. Herron and P. Moore, *J. Chem. Soc. Dalton,* 1282 (1978).
6 N. Herron and P. Moore, *J. Chem. Soc. Dalton,* 441 (1979).
7 B. Bosnich, R. Mason, P. Pauling, G. B. Robertson and M. L. Tobe, *Chem. Comm.,* 97 (1965).
8 A. Anichini, L. Fabbrizzi, P. Paoletti and R. M. Clay, *Inorg. Chim. Acta, 24,* L21 (1977).
9 N. W. Alcock, N. Herron and P. Moore, *J. Chem. Soc. Dalton,* 394 (1978).
10 N. W. Alcock, N. Herron and P. Moore, *J. Chem. Soc. Dalton,* submitted for publication.
11 E. K. Barefield, F. Wagner, A. W. Herlinger and A. R. Dahl, *Inorg. Synthesis, 16,* 220 (1976).
12 D. F. Evans, *J. Chem. Soc.,* 2003 (1959).
13 L. Fabbrizzi and P. Paoletti, *Gazzetta, 104,* 929 (1974).
14 B. Bosnich, M. L. Tobe and G. A. Webb, *Inorg. Chem., 4,* 1109 (1965).
15 S. C. Nyburg and J. S. Wood, *Inorg. Chem., 3,* 468 (1964).
16 M. J. d'Aniello and E. K. Barefield, *J. Am. Chem. Soc., 98,* 1610 (1976).
17 L. Y. Martin. C. R. Sperati and D. H. Busch, *J. Am. Chem. Soc., 99,* 2968 (1977).
18 L. Y. Martin, *Ph. D. Thesis,* Ohio State University (1974).
19 O. Bostrup and C. K. Jørgensen, *Acta Chem. Scand., 11,* 1223 (1957).
20 C. K. Jørgensen, *Acta Chem. Scand., 10,* 887 (1956).